The United Nations University

GEOTHERMAL TRAINING PROGRAMME
Orkustofnun, Grensásvegur 9,
IS-108 Reykjavík, Iceland

Reports 1995
Number 12

RESERVOIR ASSESSMENT OF THE SOUTHEAST SECTOR OF THE KAMOJANG GEOTHERMAL FIELD, INDONESIA

Doddy Satyajit Sasradipoera
PERTAMINA - Directorat Eksplorasi dan Produksi,
Divisi Panas Bumi,
Jl. Kramat Raya 59, Jakarta,
INDONESIA

ABSTRACT

A general description is given on the southeast sector of the Kamojang geothermal field. It is assumed that there is a low-permeability barrier separating the sector from the main production field. Evaluation of formation temperatures and pressures is carried out from 175 downhole measurements. A conceptual reservoir model is presented, suggesting a vapour dominated reservoir of 240-246°C initial temperature and 35-37 bars initial pressure. The reservoir is around 1 km thick and overlain by 500-1000 m thick liquid saturated caprock. The southeast sector of the Kamojang field appears to be 2-4°C hotter than the main wellfield, suggesting either the existence of an upflow zone or a low permeability volume.

Volumetric assessment for the southeast sector of Kamojang suggests a power potential of 9.5 MW_e per km^2 of the wellfield. Estimating the reservoir area to be 1.5-2.5 km^2 gives 14-24 MW_e in total. On the other hand, by using the Monte Carlo statistical approach, a 15-30 MW_e reserve estimate is obtained for the wellfield.

1. INTRODUCTION

Kamojang geothermal field has been operated by Pertamina, a state owned oil company since 1983, with the initial stage of development producing 30 MW_e utilizing steam from six wells. Two additional 55 MW_e turbines (Unit II and III) increased the capacity to 140 MW_e in late 1987 supplied from 26 wells (Sudarman et al., 1995). An additional 80 MW_e power plant is scheduled to be built in the future. In the plan it is assumed that 50 MW_e will be supplied from wells in the southeast sector of the Kamojang field, while the remaining 30 MW_e will be supplied by the northwest sector.

This report presents a reservoir evaluation study of the southeast sector of the Kamojang geothermal field. Among others, evaluations of reservoir pressures and formation temperatures are made and a conceptual reservoir model is presented. Finally, a volumetric assessment was carried out using Monte-Carlo simulation in order to estimate the reserve potential.

This report is a final part of the United Nations University Geothermal Training Programme at Orkustofnun, Reykjavík, which extended from May to October 1995.

2. GENERAL OUTLINE OF THE KAMOJANG GEOTHERMAL FIELD

The Kamojang geothermal field is located about 35 km south of Bandung, the capital city of the West Java Province, Indonesia. An active volcano (Gn. Guntur) lies about 7 km to the east of the field. An overview of the field is given in Figure 1.

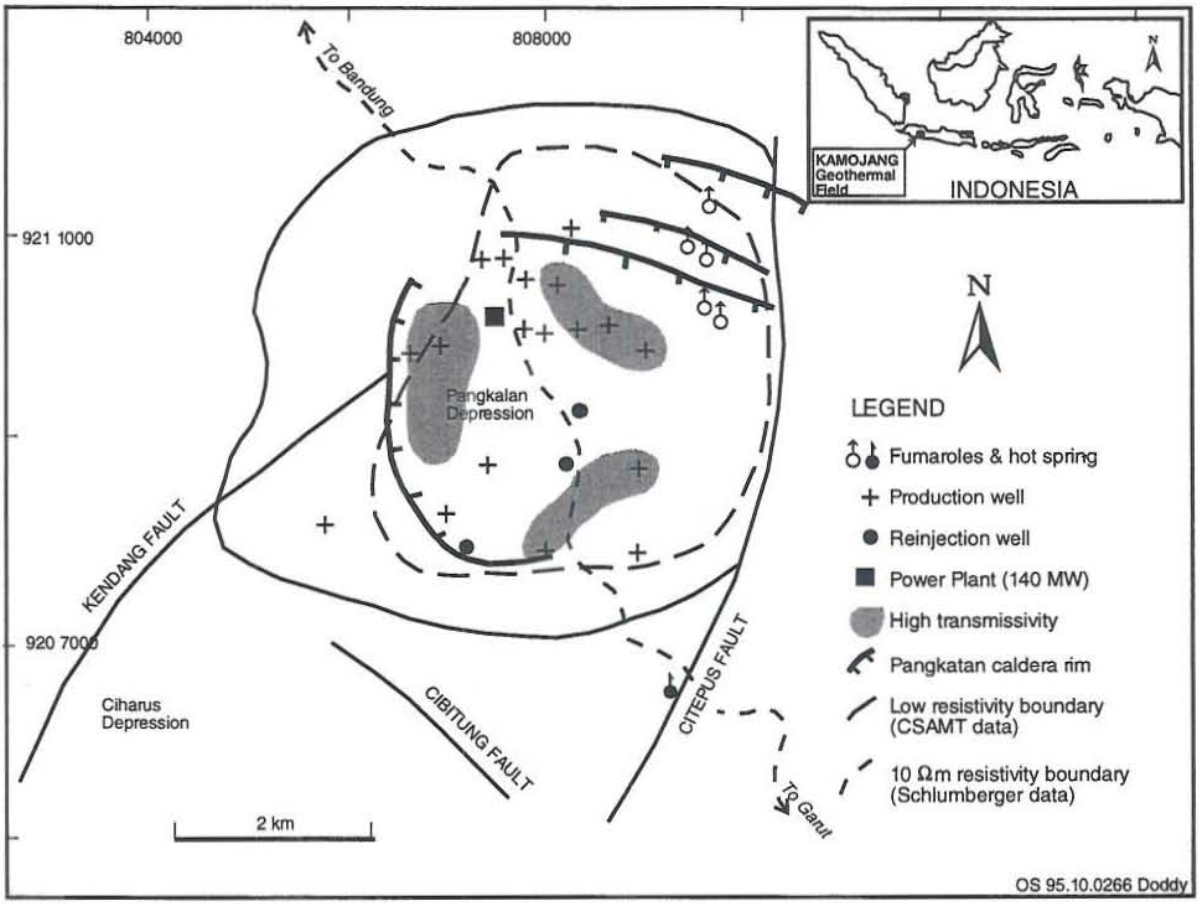

FIGURE 1: An overview of the Kamojang geothermal field showing location of wells and main geological structures (adapted from Sudarman et al., 1995)

A reservoir area of 14 km^2 has been estimated from DC-Schlumberger soundings (Hochstein, 1975) and a further field delineation of up to 21 km^2 has been determined from CSAMT studies (Sudarman et al., 1990).

The geothermal area is situated in an E-W trending Rakutak-Guntur volcanic chain at an elevation of about 1500 m a.s.l. The field is a steam dominated system, and associated with 400,000 year old Quaternary volcanic products of Pangkalan and Gandapura volcanic centres. It appears to occupy a volcanic depression created by the Pangkalan caldera rim inside the NE-SW graben formed by the Kendang fault in the west and Citepus fault in the east (Sudarman et al., 1995). The Pangkalan caldera rim, the Citepus fault and a W-E trending fault system on the northern part of the field are associated with high steam productivity (Figure 1). Two low-permeability barriers are assumed to exist in the Kamojang field, striking NW-SE and SW-NE (Figure 2). The SW-NE permeability barrier is interpreted as a "shear zone" from normal faulting observed in the area (Robert, 1988).

Several surface manifestations are found in the Kamojang area. They consist of solfataras, fumaroles, steaming ground, mud pools and hot water pools in an area of approximately 500x500 m. The chemical analysis of the hot water manifestations in Kamojang show low content of chlorine. The gas content in the steam is approximately 2% by weight, mostly CO_2 and H_2S.

The steam production is predominantly from two areas within the wellfield, in the north close to well KMJ-18 and in the northwest around KMJ-30 (GENZL, 1992). From analysis of the reservoir permeability, the Kamojang geothermal field has at least three areas of high transmissivity separated by zones of poor transmissivity (Figure 2), suggesting that the three areas are not connected (Sudarman et al., 1995). In particular, the presence of a SW-NE barrier should be stressed. The existence of this barrier is based on the low productivity observed in wells drilled there. The barrier allows one to treat the southeast sector of the Kamojang field as an independent subfield.

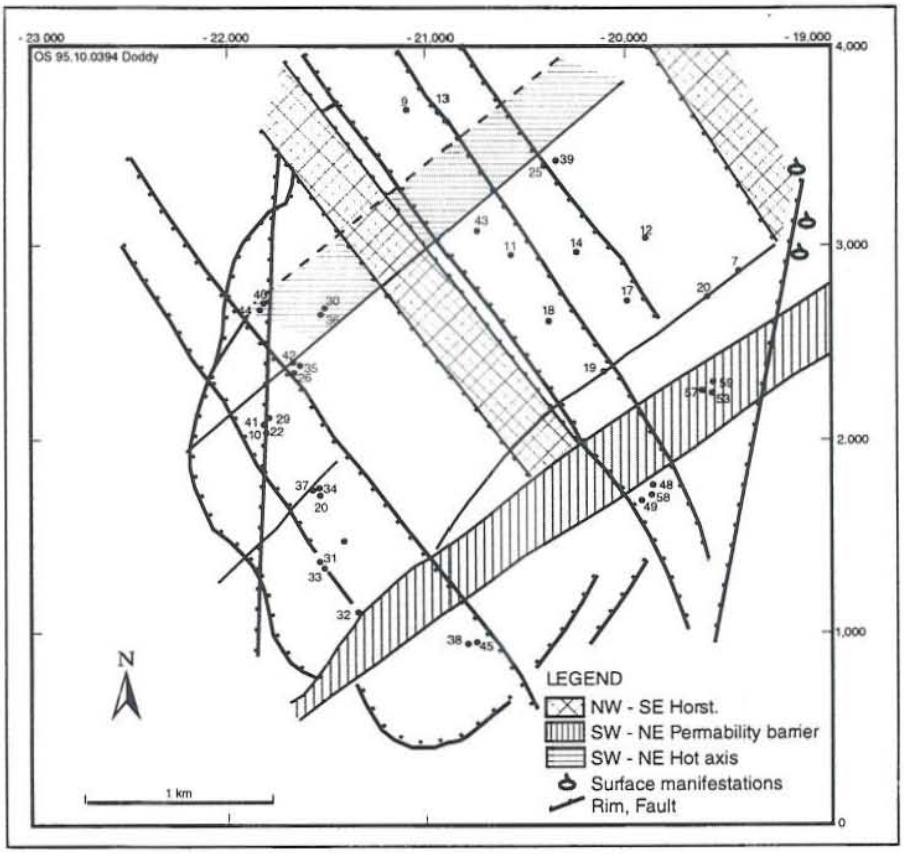

FIGURE 2: A structural map of Kamojang geothermal field, showing also location of wells (adapted from Robert, 1982)

Geothermal drilling in the Kamojang area was initiated in 1974-1975 when five exploration wells were drilled down to 700 m throughout the area. Two of these are productive, producing dry steam from shallow feed zones with temperature of 232°C at about 600 m depth (Sudarman et al., 1995). To date 59 wells have been drilled in the Kamojang geothermal field within an area of 14 km^2. Nine of the wells are located in the southeast part of the field, which is the scope of this study (Figures 1 and 2). Table 1 records general information about the wells.

TABLE 1: An overview of wells in the southeast sector of the Kamojang geothermal field (MD = measured depth)

	KMJ-38	KMJ-45	KMJ-48	KMJ-49	KMJ-53
Drill date: From	1984-06-10	1986-10-25	1989-09-26	1991-07-16	1992-10-09
To	1984-09-07	1986-12-13	1989-12-27	1991-12-09	1992-12-15
Location:					
Elevation (m a.s.l.)	1483	1483	1483	1483	1581
Surface: N-S (m)	993	995	1609	1601	2383
E-W (m)	-20821	-20813	-19821	-19816	-19638
Bottom hole: N-S (m)	738	1076	1582	1161	2611
E-W (m)	-21011	-20592	-19537	-19768	-18944
Well design:					
Kick off point (m MD)	295	700	450	400	450
Inclination	17°	27°	32°	34°	33½°
Direction	S40°W	N69°E	S79°E	S6°E	N65°E
Measured depth (m)	1441	1472	1375	1512	1300
Vertical depth (m)	1391	1386	1314	1401	1239
Casing: 9 5/8" (m MD)	1483	902	811	954	697
7" (blind)	835-1184	848-1032	763-930	905-999	651-703
7" (slotted)	1184-1441	1032-1472	830-1369	999-1510	703-1270
Status of well:	Productive	Productive	Productive	Productive	Monitoring
	KMJ-54	**KMJ-57**	**KMJ-58**	**KMJ-59**	
Drill date: From	1993-02-17	1994-02-04	1994-06-10	1994-09-05	
To	1993-05-05	1994-04-10	1994-08-21	1994-11-08	
Location:					
Elevation (m a.s.l.)	1374	1581	1483	1581	
Surface: N-S (m)	559	2392	1594	2402	
E-W (m)	-19889	-19644	-19807	-19656	
Bottom hole: N-S (m)	167	2136	1291	2871	
E-W (m)	-19306	-19492	-19511	-19376	
Well design:					
Kick off point (m MD)	450	350	370	260	
Inclination	32°	25¼°	31°	42¾°	
Direction	S66°E	S31°E	S44°E	N32°E	
Measured depth (m)	1800	1210	1350	1298	
Vertical depth (m)	1607	1145	1244	1104	
Casing: 9 5/8" (m MD)	1045	668	777	625	
7" (blind)	open hole	620-830	657-887	open hole	
7" (slotted)	8½"	831-1200	887-1277	8½"	
Status of well:	Monitoring	Heating up	Heating up	Heating up	

3. ANALYSIS OF DOWNHOLE PRESSURE AND TEMPERATURE DATA

3.1 Data sources

The well measurements used in the study have been collected over the period from 1984 to the end of 1994. A total of 79 temperature measurements and 75 pressure measurements were retrieved, stored in a PC-computer and plotted for the individual wells, both in terms of depth and time at selected depths.

The tools used for the pressure and temperature logging are mechanical Kuster probes, due to the high temperature of the wells. The accuracy is in the order of ± 3°C for temperature and ± 1 bar for pressure.

3.2 Evaluation of formation temperatures and initial pressures

The estimation of initial pressures and temperatures in the Kamojang wells is not a straight forward task due to the vapour dominated nature of the reservoir. This is reflected in the collected downhole pressure and temperature data which in general are dominated by only one feedzone in the respective well.

The evaluation of formation temperatures and initial pressures in the wells is, therefore, based on the following basic assumptions:

1. The reservoir is vapour dominated and at saturation conditions;
2. The deep well temperature and pressure can only be estimated at the depth of the major feedzone. The reservoir pressure and temperature above and below the feedzone follow vapour static gradient, corresponding to the density of steam at 240°C (0.18 bars/100 m);
3. The reservoir is overlain by a liquid dominated caprock which is characterized by the measured pressure and temperature gradient observed in the shallow well KMJ-08;
4. The caprock extends down to the depth where the caprock and the vapour static pressure curve intersect.

Well KMJ-08 was drilled in 1975 to 640 m depth. The well is vertical and non-productive. Figure 3 shows the temperature and pressure data collected. As no internal flow is taking place in the well, the initial pressure and the formation temperature are simply taken as the equilibrated measured temperature and pressure in the well. It should be noted that this is the only well in the southeast sector of Kamojang that reflects the temperature and the pressure condition in the caprock overlying the vapour dominated reservoir.

Well KMJ-38 was drilled in 1984 to a depth of 1441 m. The well is directional to the southwest. It is a good producer, and is already connected for electrical production. Figure 4 shows the observed temperatures and pressures at the major feedzone, located at 132 m a.s.l. Although the data seem scattered, an initial pressure estimate is taken as 34.2 bars, which equals the highest observed pressure. The temperature is assumed to be saturation temperature at this "match point" pressure. The formation

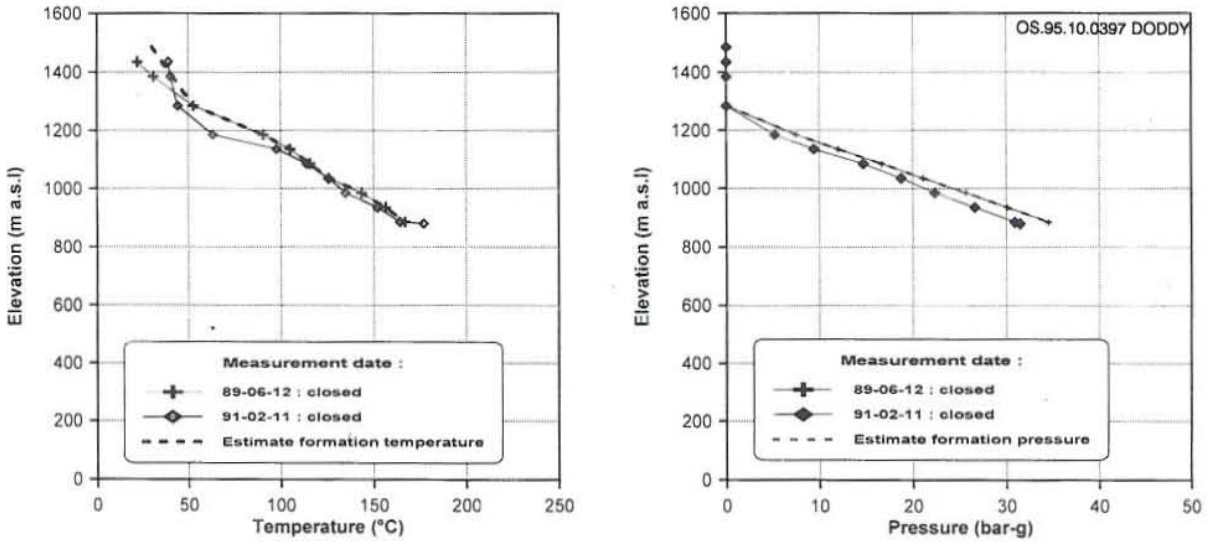

FIGURE 3: Well KMJ-08, measured and estimated formation temperatures and pressures

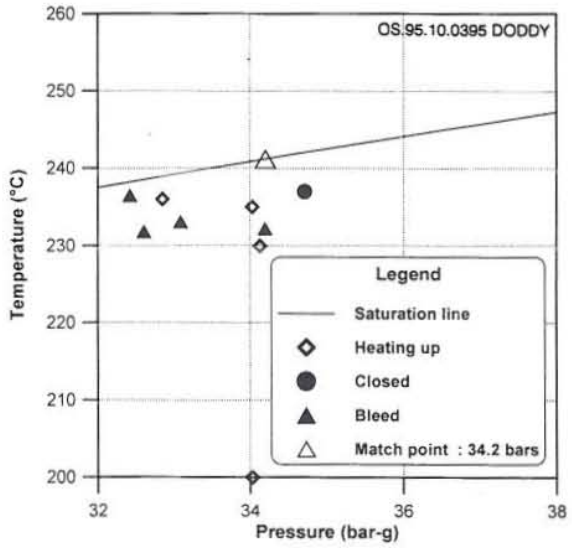

FIGURE 4: Well KMJ-38, observed pressures and temperatures at 132 m a.s.l.

temperature and the initial pressure profiles are based on this match point value, the 0.18 bars/100 m pressure gradient in the vapour static reservoir and the caprock temperature and pressure gradient observed in well KMJ-8. Figure 5 shows this estimate along with the measured downhole data.

It should be noted that during initial heating after drilling, well KMJ-38 was kept fully closed. A zone of non-condensable gas was formed in the well during this period, pressing the well fluid almost down to the major feedzone. The well temperature stayed considerably lower than the estimated formation temperature, suggesting cooler and even fully saturated conditions in the reservoir. However, the temperature data was collected only during 2 weeks of warm-up and

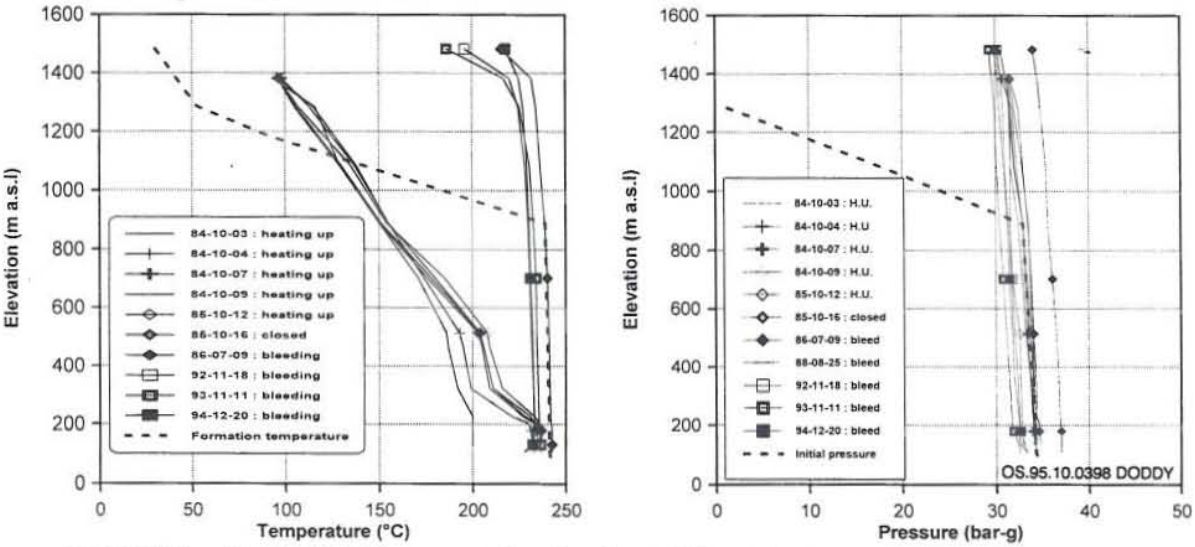

FIGURE 5: Well KMJ-38, measured and estimated formation temperatures and pressures

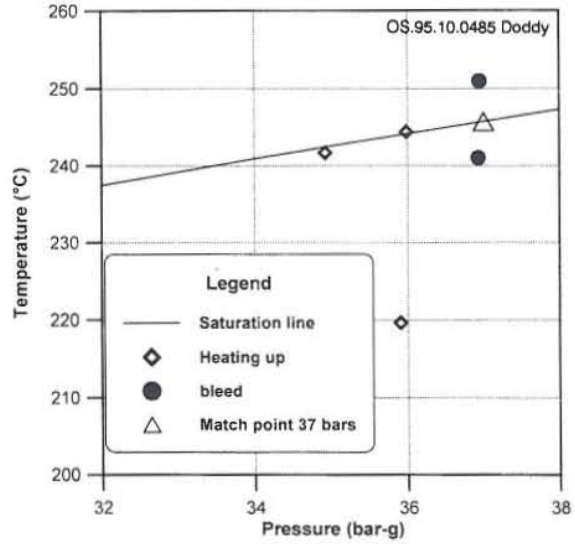

FIGURE 6: Well KMJ-45, observed pressures and temperatures at 167 m a.s.l.

therefore, may still be dominated by cooling during drilling.

Well KMJ-45 was drilled in 1986 to a depth of 1472 m and directed to N69°E. The well is productive and connected to the Kamojang power plant. Figure 6 shows the observed pressures and temperatures at 167 m a.s.l., where the major feedzone of the well is located.

The initial match point pressure is taken to be the maximum observed pressure, 37 bars. The initial pressures and the formation temperatures were evaluated using the same procedure as for KMJ-38, and presented in Figure 7 along with the measured downhole data. Again the warm-up

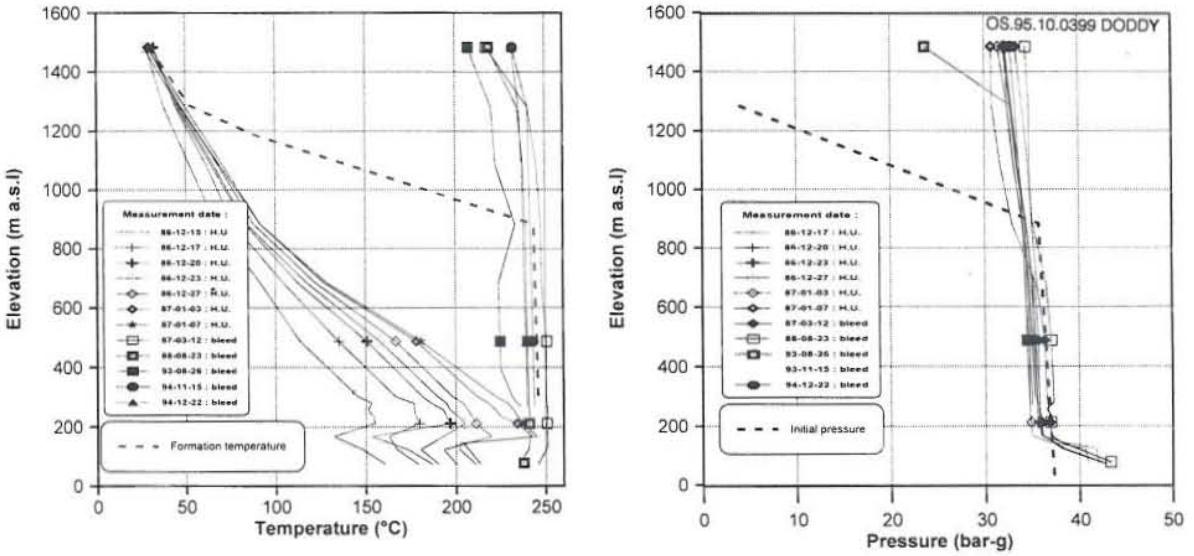

FIGURE 7: Well KMJ-45, measured and estimated formation temperatures and pressures

rate appears to be very slow during the period when the well was totally closed and full of non-condensable gas. Therefore, the formation temperature may be overestimated in the 400-1000 m a.s.l. depth interval.

Well KMJ-48 was drilled in 1989 to a depth of 1375 m a.s.l. The well is directed to S79°E and is productive but not connected to the Kamojang steam gathering system. Figure 8 shows the measured pressure and temperature data at the depth of the major feedzone (320 m a.s.l.). The match point pressure is taken as 36.5 bars, which is slightly lower than the maximum pressure observed. The initial pressure and temperature profiles with depth are estimated as before, and shown in Figure 9 together with the measured data. Note that a liquid pressure gradient is

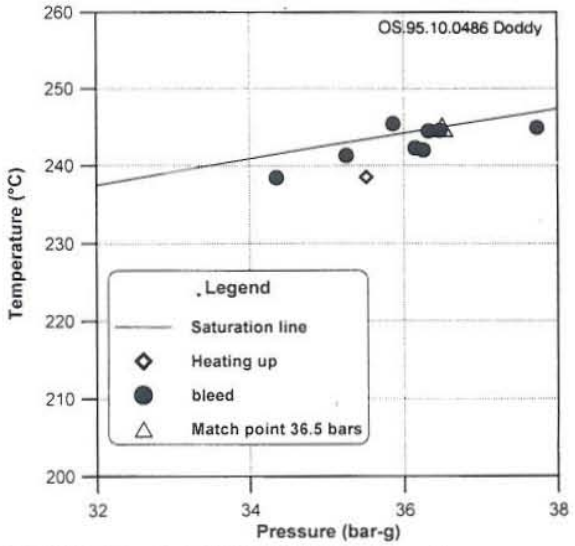

FIGURE 8: Well KMJ-48, observed pressures and temperatures at 320 m a.s.l.

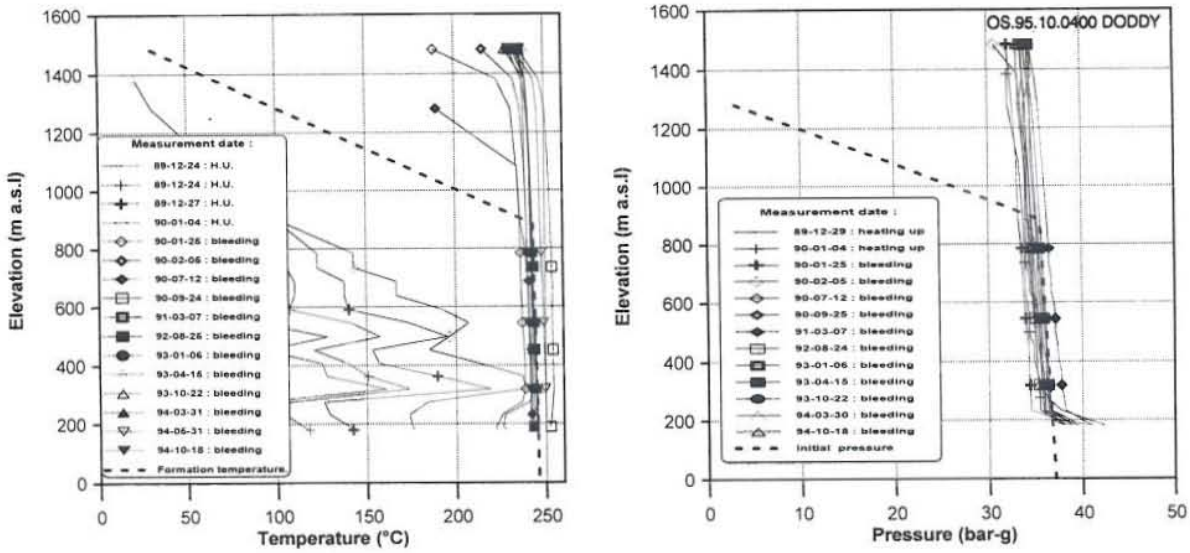

FIGURE 9: Well KMJ-48, measured and estimated formation temperatures and pressures

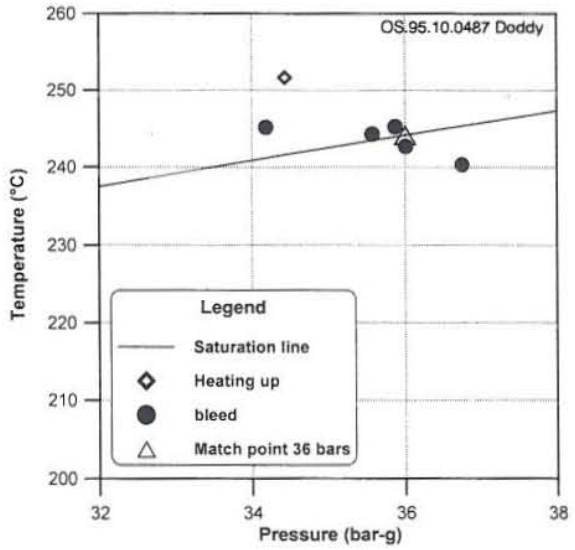

FIGURE 10: Well KMJ-49, observed pressures and temperatures at 500 m a.s.l.

measured in KMJ-48, below the major feedzone. Its presence is most likely due to circulating fluid left in this depth interval after drilling. Since the wellbore temperature is near constant at vapour-static conditions in this depth interval, the pressure is also assumed to follow vapour static conditions.

Well KMJ-49 was drilled in 1991 to a depth of 1483 m. The well is deviated to the south. It is productive but still to be connected. The measured downhole pressure and temperature data are shown in Figure 10 at the depth of 500 m a.s.l., which is the location of the best feedzone of the well. A match point value of 36 bars was obtained for the initial saturation pressure. The estimated initial pressures and formation temperatures are shown in Figure 11 together with the measured data.

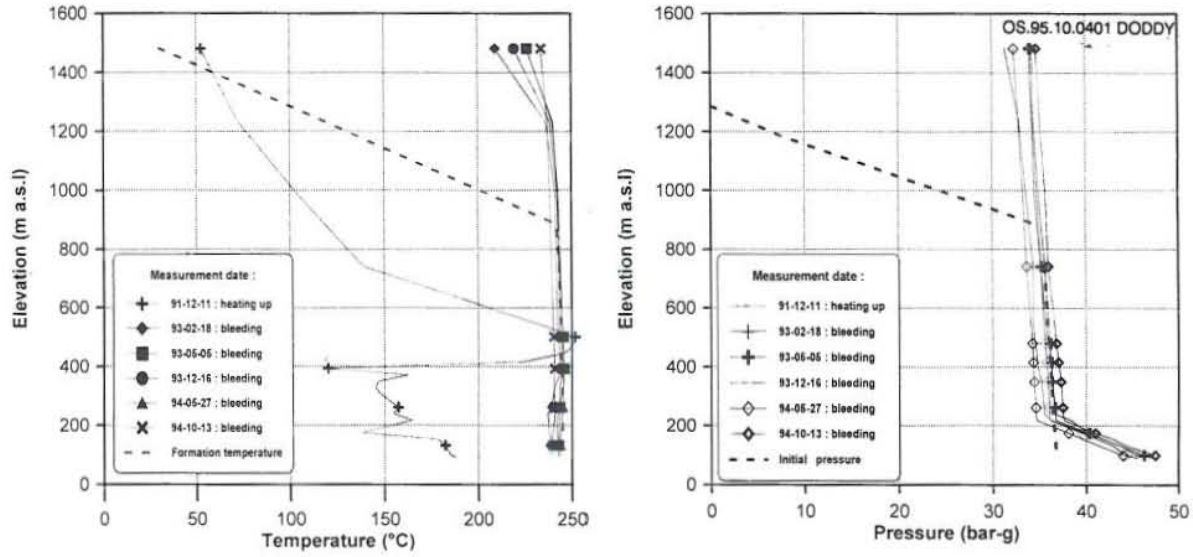

FIGURE 11: Well KMJ-49, measured and estimated formation temperatures and pressures

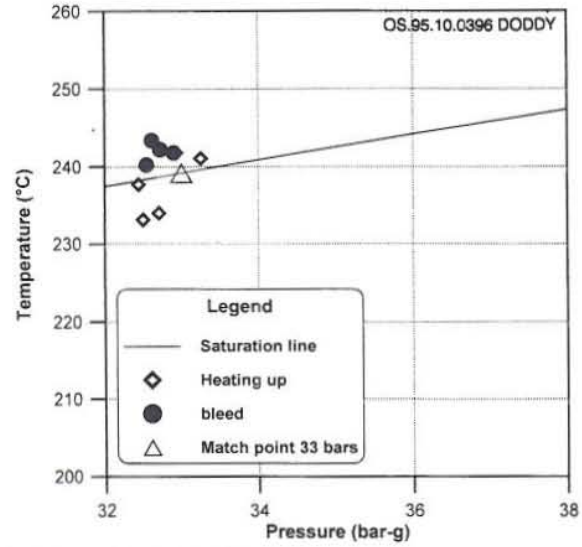

FIGURE 12: Well KMJ-53, observed pressures and temperatures at 500 m a.s.l.

Well KMJ-53 was drilled in 1992 to a depth of 1300 m and inclined to N65°E. The well is non-productive. Figure 12 shows the pressure and temperature data used to estimate the initial conditions of the well's major feedzone at 791 m a.s.l. The match point pressure is estimated as 33 bars. The associated initial pressure and formation temperature curves are shown in Figure 13 along with several downhole pressure and temperature profiles.

Well KMJ-54 was drilled in 1993 to a depth of 1800 m a.s.l. This well is deviated to S66°E. The well is characterized by low temperatures and appears, therefore, to be drilled out of the vapour dominated Kamojang reservoir (Figure 1). An

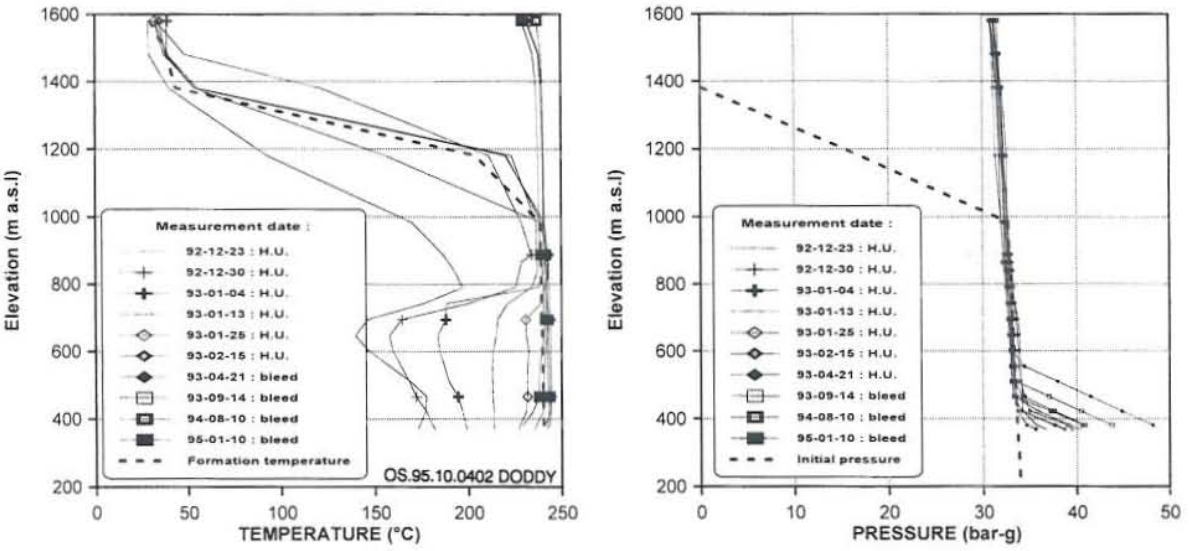

FIGURE 13: Well KMJ-53, measured and estimated formation temperatures and pressures

initial pressure of 34.1 bars and formation temperature of 190°C are estimated as bottomhole conditions (Figure 14). The formation temperature profile is simply based on maximum values of the observed temperature. The initial pressure is finally calculated using the formation temperature profile as a reference for liquid density in hydro/vapour static calculations (programme Predyp, Arason and Björnsson, 1994).

Figure 14 shows the estimated initial pressure and temperature profiles along with the measured data. The initial pressure profiles are substantially lower than the caprock pressure observed in KMJ-08 and these two profiles appear not to be connected. This low pressure at depth suggests that the Kamojang reservoir is in hydraulic connection to outer and colder, liquid dominated regions. A detailed analysis of the initial status of well KMJ-54 is therefore of great interest for studies regarding natural recharge to the Kamojang reservoir.

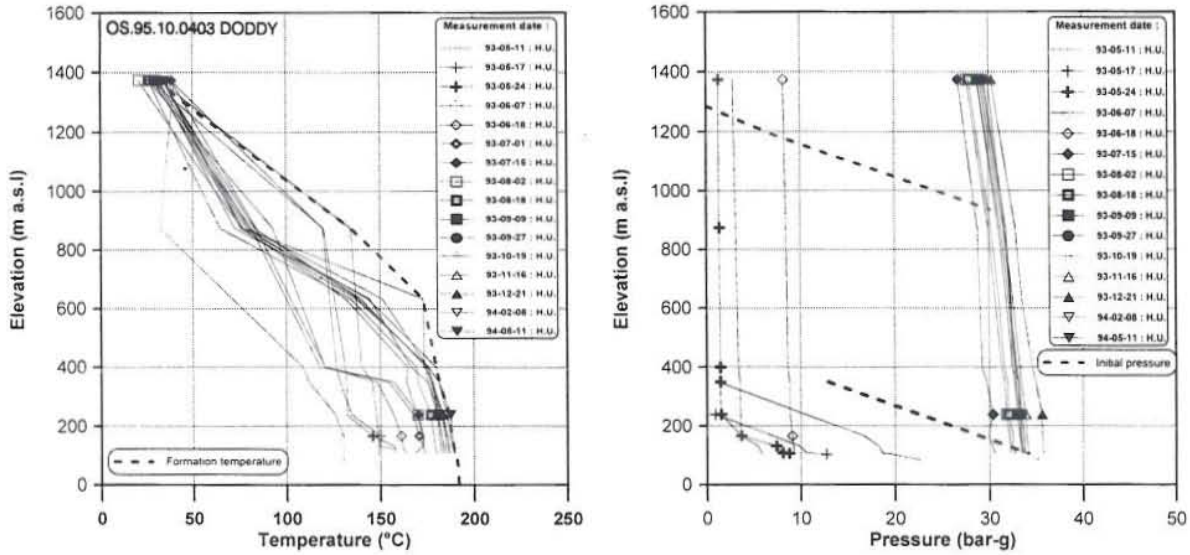

FIGURE 14: Well KMJ-54, measured and estimated formation temperatures and pressures

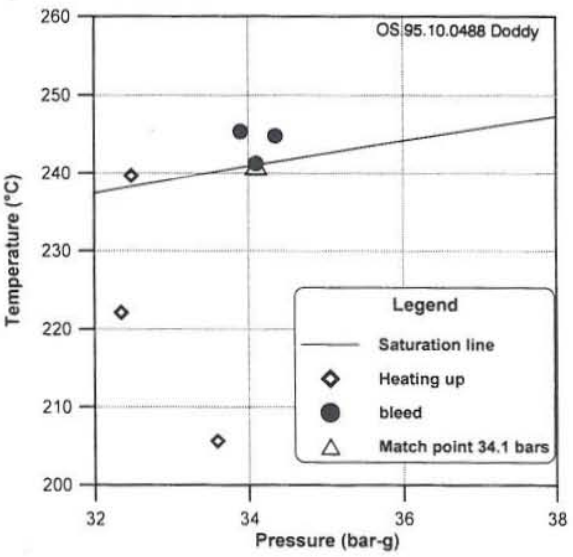

Well KMJ-57 was drilled in 1994. The well is 1210 m deep and directed to S31°E. Production information for well KMJ-57 was not available for this study. Figure 15 shows the observed pressures and temperatures at 746 m a.s.l., where the best feedzone of the well is located. A match point pressure of 34.1 bar-g is suggested. The estimated profiles of initial pressure and formation temperature are shown in Figure 16 together with the measured downhole data in the well.

FIGURE 15: Well KMJ-57, observed pressures and temperatures at 746 m a.s.l.

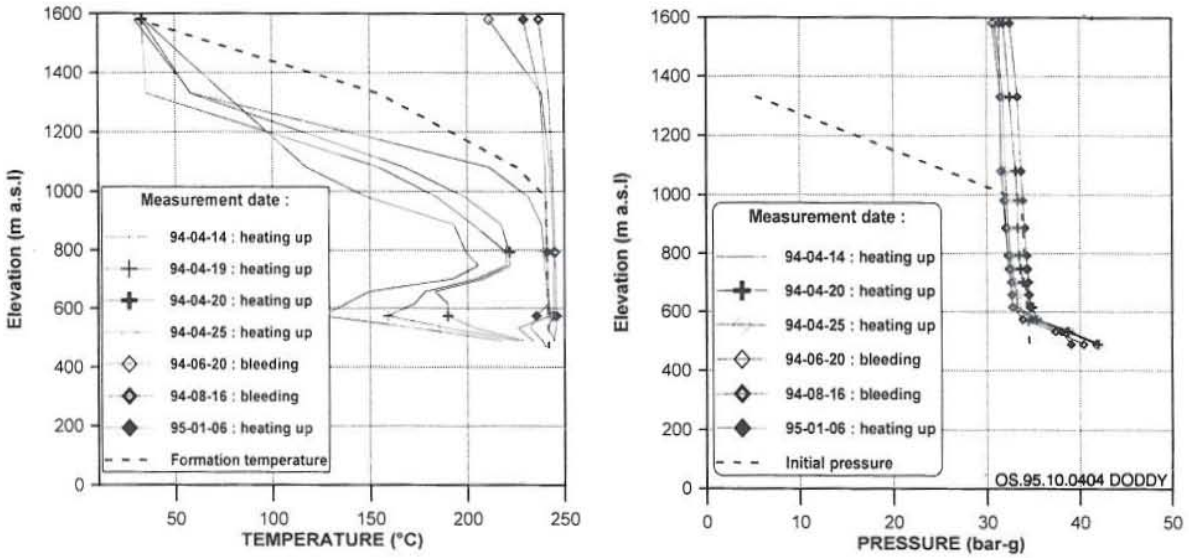

FIGURE 16: Well KMJ-57, measured and estimated formation temperatures and pressures

3.3 Initial temperature and pressure distribution

It is of interest to draw the initial pressure and formation temperature curves presented here in cross and plane sections. Figure 17 shows the formation temperature at 300 m a.s.l. Although the southeast sector of the wellfield is the scope of this study, formation temperature data from another study are also shown in the figure (Barnett, 1988). The depth of 300 m a.s.l. was selected due to the fact that most wells have their major feedzones close to this depth, resulting therefore in the most accurate contouring. The pressure distribution is not shown here, but follows the same contouring as the temperature, due to the saturation conditions of the reservoir.

Two major structures are evident in the proposed temperature distribution, a channel of decreasing reservoir temperature (and pressure due to boiling at this depth) towards northeast where fumaroles and steaming ground exist. This can be explained as a zone of higher reservoir permeability. Another

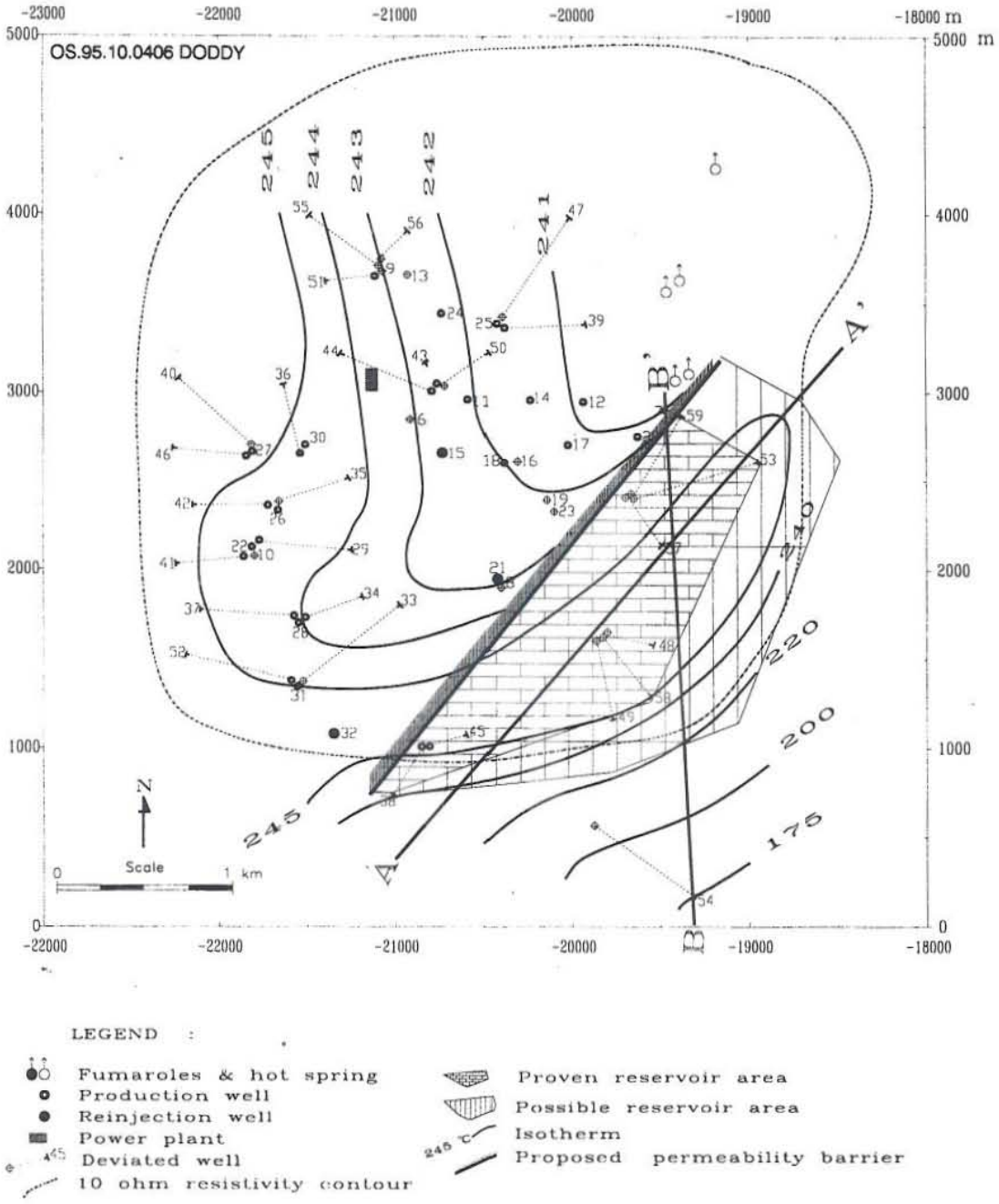

FIGURE 17: Map of the Kamojang field showing the location of the wells, formation temperature contours at 300 m a.s.l., and proven and possible reservoir areas of the southeast sector

striking feature is a hot zone of temperature >245°C, also parallel to the barrier and located within the southeast sector of the Kamojang field. The exact nature of this anomaly is not known, but can be explained as either a hot upflow zone or a low permeability volume.

Figure 18 shows the formation temperature in two cross-sections in the southeast sector at the Kamojang field. Cross-section A-A' is drawn parallel to the proposed permeability barrier, but section B-B' perpendicular to it. The A-A' sections present rather uniform lateral temperature distribution, whereas the B-B' section identifies a reservoir volume of temperature above 240°C, which is bounded to the south.

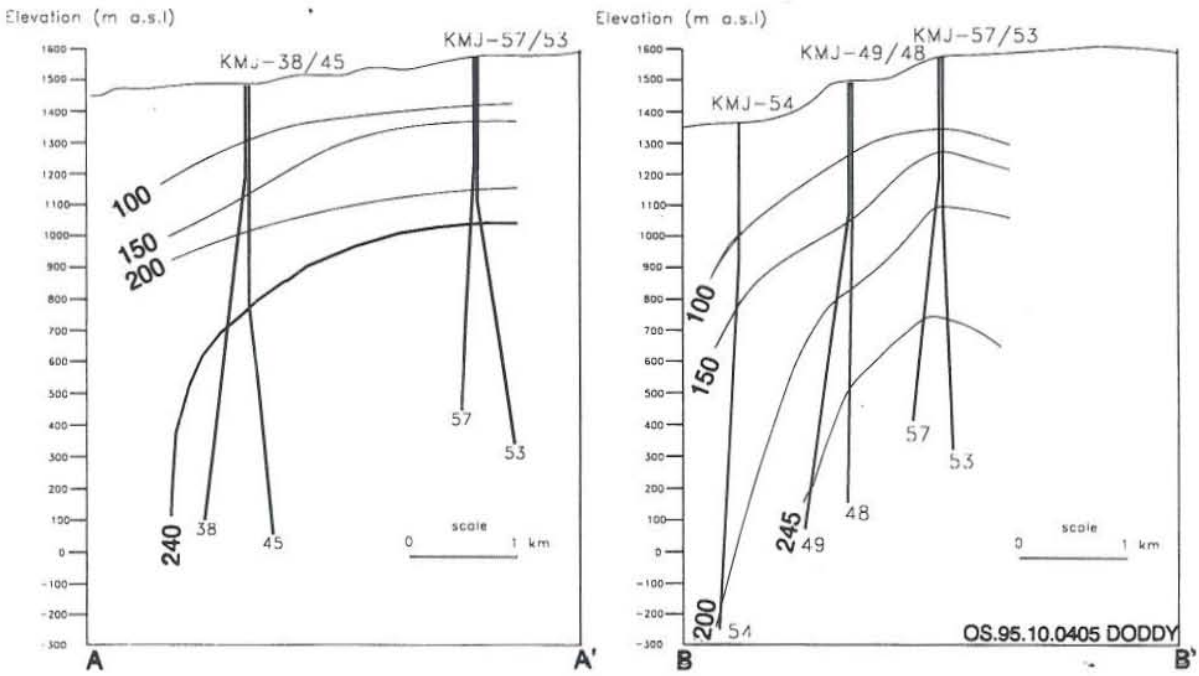

FIGURE 18: The Kamojang field, southeast sector; formation temperature cross-sections, a) A-A'; b) B-B'; locations are shown in Figure 17

3. 4 A conceptual reservoir model

The initial pressure and temperature data presented here allow presentation of a conceptual reservoir model for the southeast sector of Kamojang field. The model is shown schematically in Figure 19.

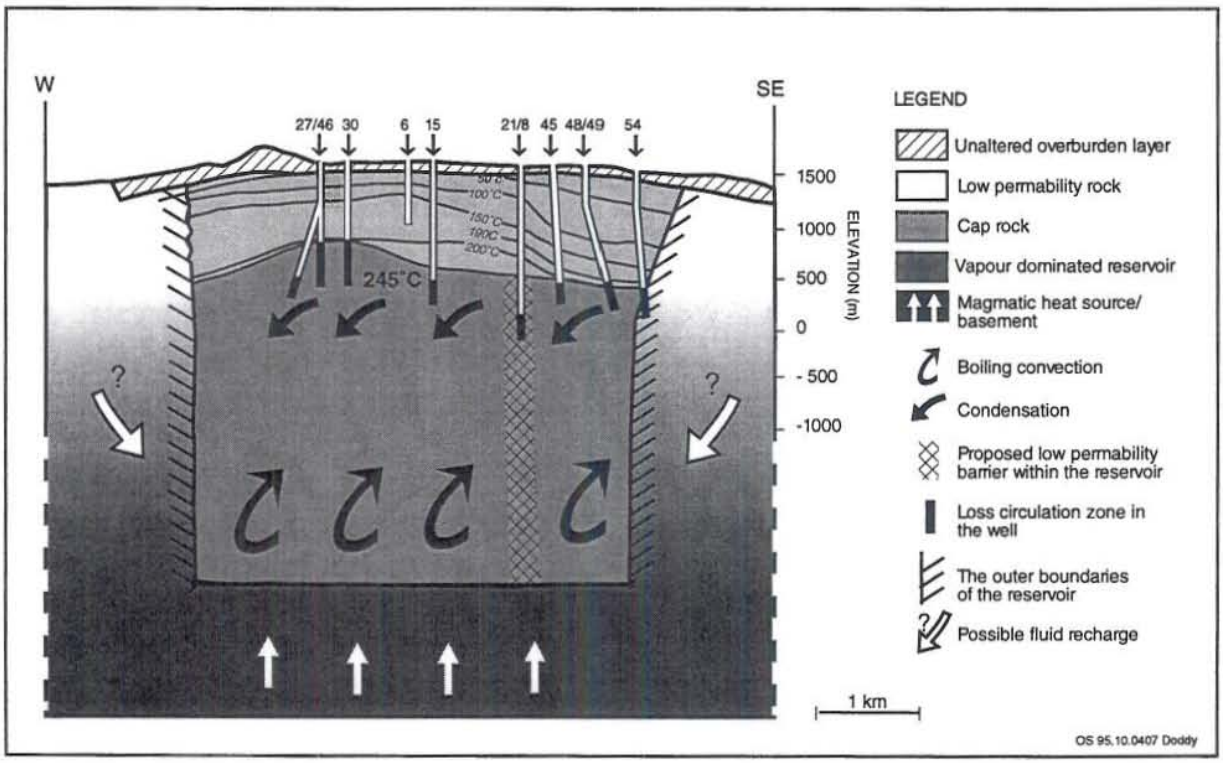

FIGURE 19: A conceptual reservoir model of the Kamojang geothermal field (modified from Sudarman and Hochstein, 1983)

The reservoir is associated with a graben depression, bounded by the Kendang and the Citepus faults. A low-permeability caprock of 500-1000 m thickness is covering a vapour-dominated reservoir of 240-246°C temperature. A low-permeability barrier is dividing the southeast sector from the main wellfield. Reservoir temperature appears to be 2-4°C higher on the southeast side of the barrier. The vapour-dominated reservoir is convecting the steam upwards, it is being condensed at the caprock interface, and the condensed liquid migrates downwards again (heat pipe).

The low pressure witnessed in well KMJ-54 suggests that the reservoir is connected to colder, fully liquid saturated boundaries, which may recharge some fluid to the reservoir. A heat flow from depth takes place into the reservoir, possibly originating from the cooling of intrusions and dykes. The depth to the lower boundary of the convecting vapour dominated reservoir is not known.

4. GEOTHERMAL RESOURCE ASSESSMENT

4.1 Volumetric analysis

The concept of volumetric assessment estimates the "stored heat" contained in the subsurface fluids and rocks of a geothermal reservoir, assuming a homogenous and no recharge (closed) reservoir. It is a limited method for rough estimation of the power potential of a geothermal reservoir. The equations for estimating the total heat available from a reservoir volume (Sarmiento, 1993)

$$E_s = E_r + E_f \tag{1}$$

$$E_r = (1 - \phi)\, \rho_r\, C_r\, V\, (T_I - T_R) \tag{2}$$

$$E_f = \phi\, V\, ([(1 - S_w)\, \rho_s h_s + S_w\, h_w\, \rho_w]_I - [\rho_s h_s]_R) \tag{3}$$

where

$E_{s,\,r,\,f}$	= Stored heat in the system, rock and fluid;
V	= Reservoir volume;
S_w	= Water saturation;
ϕ	= Rock porosity;
C_r	= Rock heat capacity;
$\rho_{r,\,f}$	= Density of rock and fluid;
$h_{s,\,w}$	= Steam and water enthalpy;
$\rho_{s,\,w}$	= Steam and water density;
I	= Initial conditions (245°C);
R	= Reference conditions at abandonment temperature (180°C);
$T_{I,\,R}$	= Initial and abandonment reservoir temperature (°C).

The equations above assume that there is sufficient heat contained in the reservoir rock to boil all the in situ liquid to steam. The assumption can be checked by comparing the heat energy lost by the reservoir rocks with that required to evaporate the liquid water. For a vapour dominated reservoir with immobile water, the reservoir rock temperature will fall as it evaporates the water. Grant et al. (1982) showed that the dry-out temperature (temperature at which reservoir liquid content drops to zero) is given by the energy balance:

$$\phi V S_w \rho_w (h_s - h_w) = (1 - \phi) V \rho_r C_r (T_0 - T_D) \quad (4)$$

or

$$T_0 - T_D = \phi S_0 \frac{[\rho_w (h_s - h_w]_0}{(1 - \phi) \rho_r C_r} \quad (5)$$

where

T_0 = Reservoir temperature before exploitation;
T_D = Dry-out temperature.

Using Equation 5 and an estimated liquid saturation of approximately 25%, the dry out temperature is 232°C. Therefore boiling and heat transfer from the rocks to the water will continue until the reservoir temperature reaches 232°C and the water has been evaporated. After the reservoir reaches the dry-out temperature, extraction of fluid will rapidly reduce the reservoir pressure and the steam will become superheated. If additional water were available it would be possible to continue the boiling and steam production until the rock temperature fell to 180°C (Barnett, 1988). This additional water may become applicable either by natural recharge or by injection.

The mathematical equation used in estimating the reserve potential of the southeast sector of the Kamojang field is:

$$Reserve\ (MW_e) = \frac{Stored\ heat \times Recovery\ factor \times Plant\ efficiency}{Plant\ load \times Life\ time} \quad (6)$$

From Equations 2 and 3, the stored heat in the rock is 2.95×10^{17} Joule and the stored heat in the fluid is 3.25×10^{16} Joule. Figure 18 suggests a reservoir area of 2 km^2 and the reservoir thickness is assumed 1 km from the initial temperature analysis (Figure 19). Assuming a 25% recovery of the stored heat and 25 years of production for the total reserve, this gives

$$Reserve\ (MW_e) = \frac{3.27 \times 10^{17} \times 25\% \times 16.4\%}{0.9 \times 25\ years} = 19\ MW_e$$

The above estimate equals a 9.5 MW_e power capacity per km^2, which is slightly lower than in previous studies that have been performed for the Kamojang geothermal field. They report values of 10-16 MW_e/km^2, depending on the natural recharge (Barnett, 1988; GENZL, 1992).

4.2 Monte Carlo simulation

Reserve estimation involves several uncertainties for determining the rock and the reservoir properties. Many of these parameters are poorly known and difficult to measure. Some quantities such as porosity and permeability of the host rock and their distribution can never be known exactly. To deal with the parameters used in the reserve estimation with some uncertainties, a method called Monte Carlo has been proposed (Sarmiento, 1993). The Monte Carlo simulation deals with the complex scenario that describes the mathematics of known parameters but with uncertainty or probability distribution. A random number

generator then solves the algorithm relating the uncertainty distribution by randomly accessing the values from each distribution individually in iteration.

The parameters that are used in the calculation are shown in Table 2. The minimum reservoir area used in the calculations is 1.5 km^2, which is proved by the drilling and up to 2.5 km^2 as the maximum (Figure 17). The thickness of the reservoir is allowed to range between 500 and 1500 m. The present Kamojang electrical power plant efficiency is 16.4% (Gomaa, 1994), that is 6.1 x 10^6 W are required to produce 1 MW of electricity. The recovery factor used in the calculation is 25%. There is no theoretical justification of using this value. The recovery factor is controlled by permeability structure and recharge characteristics. As an example, the value of 100% is assumed for a complete recharge of a liquid dominated system and 10% applies for no recharge and limited supply of liquid into a vapour dominated system (Gomaa, 1994). The porosity distribution is assumed to follow a log normal distribution in accordance with statistics obtained in core studies (Sarmiento, 1993).

TABLE 2: Monte Carlo analysis of the Kamojang geothermal field, best guess values and their probability distribution

Parameter	Best guess (model)	Probability distribution		
		Type	Minimum	Maximum
Area (km^2)	2	Normal	1.5	2.5
Reservoir thickness (m)	1000	Triangular	500	1500
Rock density (kg/m^3)	2640	Triangular	2508	2772
Porosity (%)	7	Log normal	-	-
Recovery factor (%)	25	Triagular	14	32
Rock specific heat (J/kg°C)	1000	Normal	950	1050
Average reservoir temperature (°C)	240	Normal	235	245
Water saturation (%)	25	Triangular	20	30
Water density (kg/m^3)	-	Table f(T)	-	-
Water enthalpy (kJ/kg°K)	-	Table f(T)	-	-
Steam density (kg/m^3)	-	Table f(T)	-	-
Steam enthalpy (kJ/kg°K)	-	Table f(T)	-	-
Plant efficiency (%)	16.4	Normal	15.4	17.4
Plant life (years)	25	Triangular	20	30
Load factor	0.8	Triangular	0.8	1.0
Abandonment temperature (°C)	180	Constant	-	-

Equation 6 is the governing equation of the Monte Carlo reserve calculations. After all the properties in the equation have been assigned their probability character, a matrix of 15 x 1000 element was set up in a Microsoft EXCEL spreadsheet. Each line of the matrix contains parameters for a single computation of the energy reserve. By repeating these calculations 1000 times, simultaneously taking into account the probability of the various parameters, a statistical distribution of the reserve is obtained. Figure 20 presents the outcome of the calculations as a histogram.

From the frequency distribution of the reserve estimate, the histogram indicates a reserve range of 10 to 55 MW_e. The cumulative frequency curve shown in Figure 20 indicates that the most likely value of the reserve (median) is 25 MW_e and there is less than 10% chance of the reserve being less than 10 MW_e or more than 55 MW_e. The calculations above use a reservoir area estimate between 1.5 and 2.5 km^2. This means that in order to develop a 55 MW_e power plant, the minimum wellfield area has to be on the order of 5 km^2. Thus it appears that an additional area of the resource has to be proven in order to realise the planned increase in future production.

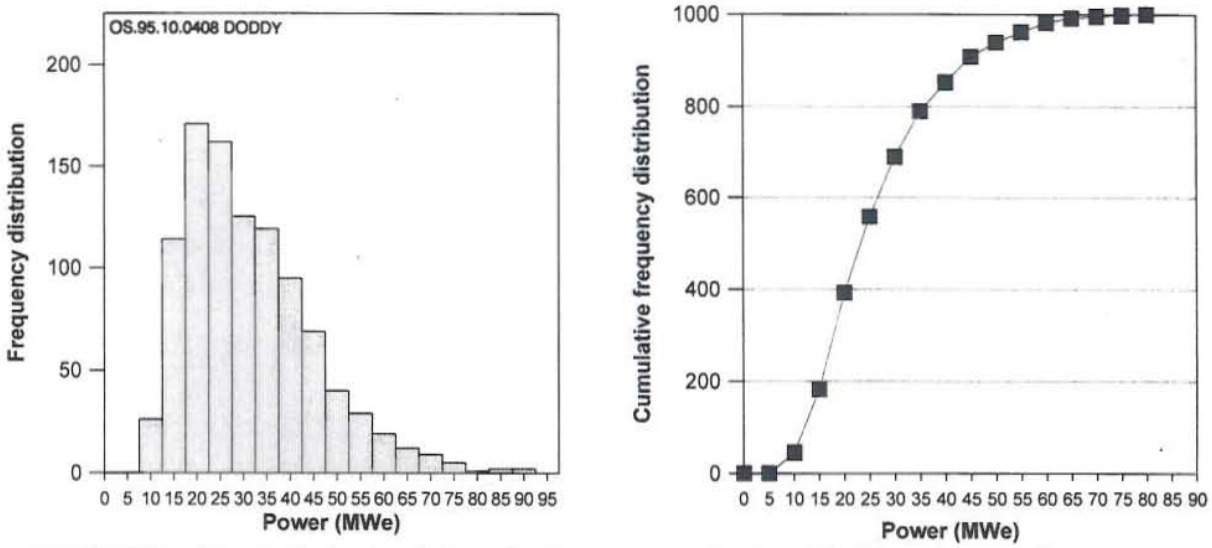

FIGURE 20: Monte Carlo simulations for the reserve estimate of the Kamojang southeast sector

5. FIELD RESPONSE TO PRODUCTION

Wells KMJ-38 and 45 have been producing since August 1987 with the initial operational well-head pressure of 15.8 bars and 17.3 bars producing 9 and 13 kg/s of steam, respectively. In the Kamojang field, wells are generally operated at constant flowrates and the wellhead pressure is adjusted in order to maintain the constant flow. Currently, these two wells are producing with the operational well-head pressure of 11.7 and 10.7 bars with flowrates of 7.7 and 6.9 kg/s of steam.

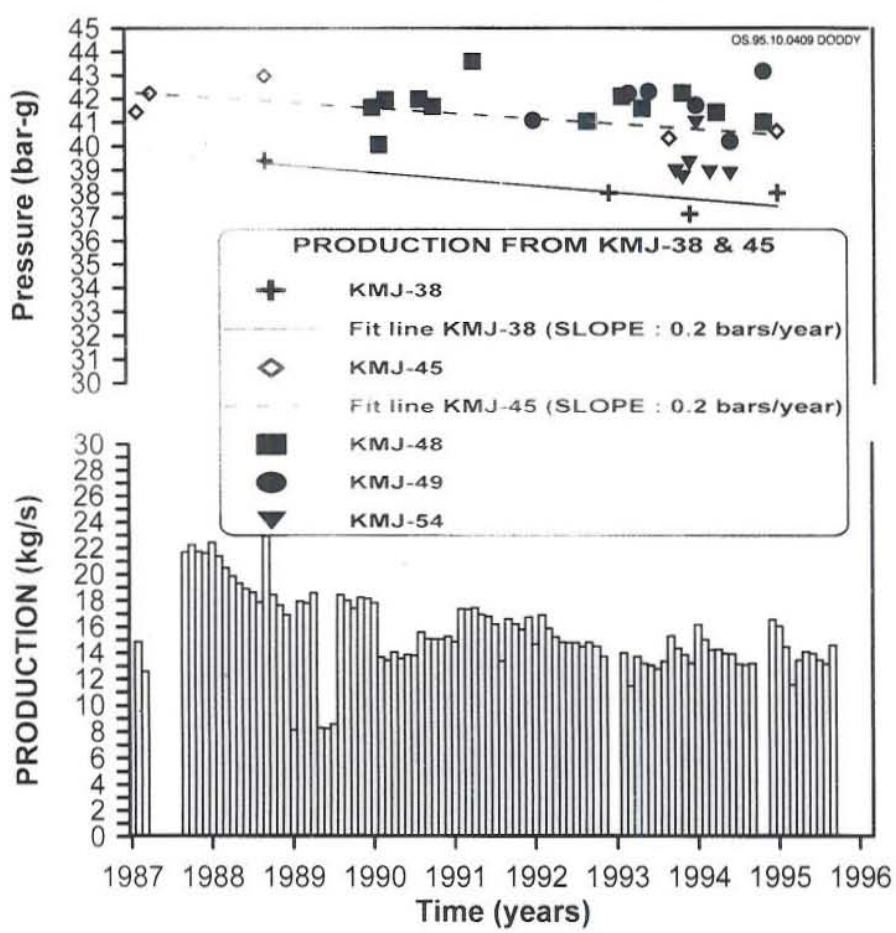

FIGURE 21: Monthly production from the Kamojang wells KMJ-38 and 45, and reservoir pressure history at 300 m a.s.l.

Figure 21 shows the downhole pressure history for all the wells in the southeast sector at 300 m a.s.l. A trend of pressure decline is seen in the downhole data for the two production wells. The pressure drawdown rate is around 0.2 bars/year for these

wells, and the total drawdown since 1987 is in the order of 1.5 bars. This decline in the reservoir pressure may explain the reduction in total flowrates also shown in Figure 21. However, wells KMJ-48, 49 and 54 appear to be stable in pressure. Reservoir pressure drawdown, due to production, seems therefore only to be visible in the vicinity of the producing wells. The stable reservoir pressure mentioned above also indicates that the permeability barrier, shown on Figure 2, is real as declining reservoir pressures have been measured at least locally in the main Kamojang wellfield (GENZL, 1992).

6. CONCLUSIONS AND RECOMMENDATIONS

The objective of the study presented in this report is to estimate the power potential of the southeast sector of the Kamojang field. Based on analysing available data, the main conclusions and recommendations of this report are:

1. Downhole pressure and temperature data from 7 wells have been analysed and initial pressure and formation temperature profiles defined.

2. Pressure and temperature distribution at 300 m a.s.l. suggest two major structures within the Kamojang wellfield. They are a channel of decreasing pressure and temperature towards northeast where fumaroles and hot grounds exist on the surface. The other structure appears to follow the southeast side of a proposed low-permeability zone in the wellfield. This structure is characterized by 2-4°C higher reservoir temperature than on the northwest side of the barrier and can be explained either as an upflow zone or a volume of low permeability.

3. A similar conceptual reservoir model is proposed for the southeast sector of the Kamojang wellfield as in the northwest side. The reservoir is vapour dominated with temperature of 241-246°C, and covered by 500-1000 m thick caprock. The reservoir appears to be bounded to the southeast due to the low temperature observed, but the nature of the reservoir boundaries to the east and south are not known due to the lack of wells drilled there.

4. The estimated reserve potential from volumetric calculation is 9.5 MW_e per km^2 of the wellfield. The most critical parameters in the calculations, like porosity and initial liquid saturation of the pores are poorly known. These parameters have to be analysed, for example by using a combination of core data and downhole lithological logging.

5. The Monte Carlo statistical analysis applied here, suggests a power potential for the southeast sector of the Kamojang field between 10 and 55 MW_e, with the best guess as 25 MW_e . For supplying enough steam to the planned 50 MW_e power plant, a larger reservoir area needs to be defined. Therefore an exploration drilling programme should be planned in order to find an additional reservoir area to support the new power plant.

6. An annual pressure decline of 0.2 bars can be seen in the downhole pressure from the two producing wells in the southeast sector of Kamojang. The drawdown is most likely due to the current exploitation. However, the accuracy of measured reservoir pressure available in this study is not sufficient to predict the long term behaviour of the reservoir with any confidence. Accurate monitoring of the reservoir pressures is essential to the analyse pressure drawdown in the field.

7. Geothermal reservoir engineering work should be included in the feasibility study for future development. A 3-D numerical simulation should be carried out in order to estimate the future performance of the reservoir and also to understand better the nature of the Kamojang reservoir.

ACKNOWLEDGEMENTS

I would like to express my gratitude to Dr. Ingvar B. Fridleifsson, the director of the UNU Geothermal Training Programme for making my Fellowship possible, and special thanks to Mr. Lúdvík S. Georgsson, Súsanna and Margrét Westlund for providing excellent attention and work conditions during the training. I sincerely thank Mr. Grímur Björnsson and Mr. Benedikt Steingrímsson, my advisors, for patient guidance during all the stages of the preparations of this report and allowing me to receive the benefits of their experience and knowledge which made the completion of this report possible. Finally, I would like express my gratitude to Pertamina (National state oil, gas and Geothermal Company/Ministry of Mining and Energy of Indonesia) for the permission to attend this programme.

REFERENCES

Arason, P., and Björnsson, G., 1994: *ICEBOX*. 2nd edition, Orkustofnun, Reykjavík, 38 pp.

Barnett, B., 1988: *Reservoir assessment of the Kamojang geothermal field*. GENZL/SMS, an internal report submitted to Pertamina, Indonesia, 25 pp.

GENZL, 1992: *Reservoir review and simulation of the Kamojang field relating to production, decline and steam supply for an additional 1x55 MW_e unit.* An internal report submitted to Pertamina, Indonesia, 38 pp.

Gomaa, A.A., 1993: *Assessment of the geothermal reserve*. Indonesian Geothermal Association, unpublished lecture notes.

Grant, M.A., Donaldson, I.G., and Bixley, P.F., 1982: *Geothermal Reservoir Engineering*. Academic Press, New York, 369 pp.

Hochstein, M.P., 1975: Geophysical exploration of the Kawah Kamojang geothermal field, West Java. *Proceedings of the 2nd U.N. Symposium on the Development and Use of Geothermal Resources, San Francisco, Ca., 2,* 1049-1058

Robert, D., 1982: *The geothermal field of Kamojang.* Pertamina/Beicip, report.

Robert, D., 1988: *Subsurface study on the optimization of the development of Kawah Kamojang geothermal field.* Beicip/Geoservices, report.

Sarmiento, Z.F., 1993: *Geothermal development in the Philippines*. UNU, G.T.P., Iceland, report 2, 99 pp.

Sudarman, S., and Hochstein, M.P., 1983: Geophysical structure of the the Kamojang geothermal field (Java). *Proceedings of the 5th New Zealand geothermal workshop, University of Auckland,* 225-230.

Sudarman, S., Boedihardi, M., Pudyastuti, K., and Bardan, 1995: Kamojang geothermal field: 10 year operation experience. *Proceedings of the World Geothermal Congress 1995, Florence, Italy, 3,* 1773-1777.

Sudarman, S., Ibrahim, L.I., and Prijanto, 1990: Geothermal field boundary delineation with CSAMT; the Kamojang case. *11th PNOC-EDC Geothermal Conference, Tongonan, Philippines.*